Determination of Thermal Diffusivities, Thermal Conductivities, and Sound Speeds of Room-Temperature Ionic Liquids by the Transient Grating Technique

Clifford Frez* and Gerald J. Diebold

Department of Chemistry, Brown University, 324 Brook Street, Providence, Rhode Island 02906

Chieu D. Tran and Shaofang Yu

Department of Chemistry, Marquette University, P.O. Box 1881, Milwaukee, Wisconsin 53201

We report measurements of thermal diffusivity of several room-temperature ionic liquids (RTILs) using the transient grating method. Measurements are carried out using ionic liquids with small concentrations of an inert dye that is excited by the 532 nm output of a Nd:YAG laser in a grating with a fringe spacings of (92 and 104) μm. The experiments give thermal diffusivities from which thermal conductivities can be determined, sound speeds, and acoustic damping parameters for seven ionic liquids. In this study, we have used combinations of the cation 1-butyl-3-methylimidazolium ($[BMIm]^+$) with the anions tetrafluoroborate ($[BF_4]^-$), hexafluorophosphate ($[PF_6]^-$), and bis(trifluoromethylsulfonyl)imide ($[Tf_2N]^-$) and combinations of the anion $[Tf_2N]^-$ with the cations 1-ethyl-3-methylimidazolium ($[EMIm]^+$), 1-pentyl-3-methylimidazolium ($[PMIm]^+$), 1-hexyl-3-methylimidazolium ($[HMIm]^+$), and 1-octyl-3-methylimidazolium ($[OMIm]^+$) to determine the effect of anion and cation on the thermophysical properties of the RTILs. Results obtained indicate that the anion exerts a strong influence not only on the sound speed but also on the thermal diffusivity and acoustic damping of the RTILs. For RTILs with the same cation $[BMIm]^+$, changing the anion from $[BF_4]^-$ to either $[PF_6]^-$ or $[Tf_2N]^-$ leads to decreases in the sound speed, thermal diffusivity, and thermal conductivity. The size of the cation, however, does not significantly influence the sound speed or the thermal diffusivity of the RTILs.

Introduction

Room-temperature ionic liquids (RTILs) are organic salts that are liquid at room temperature and that have unique chemical and physical properties, including stability on exposure to air and moisture, a high solubility power, and extremely low vapor pressure. Because of these properties, they can serve as a "green" recyclable alternative to the volatile organic compounds that are traditionally used as industrial solvents. In the laboratory, RTILs have successfully been used in a broad spectrum of applications, including replacing traditional organic solvents in organic and inorganic syntheses, solvent extractions, liquid−liquid extractions, electrochemical reactions, and as a medium for enzymatic reactions.[1−8]

The majority of studies have focused on synthesizing RTILs with new anions and cations and determining their chemical properties. Unfortunately, information on the RTILs including their physical properties and the relationships between structure and physical properties is not widely available despite their superior physical properties, which make them suitable not only as green solvents but also as high-performance fluids for use in a wide range of engineering and materials science applications, such as high-pressure and high-temperature[1−8] lubricants. It is probable that industrial applications of RTILs in chemistry, engineering, and material processing are limited because of the paucity of data on their physical properties.

Transient grating method is a noncontact method of probing both photothermal and photoacoustic changes in density[9−11] and can be used to determine thermophysical properties of solids, liquids, and gases. The method is based on the formation of a series of nodes and antinodes in the electric field of the laser beams in space generated by intersecting two coherent, pulsed laser beams, referred to as "pump" beams, in a weakly absorbing sample.[9−15] Following absorption of the laser radiation, the excited chromophore typically decays on a fast time scale with respect to the laser pulse width depositing the absorbed optical energy in the fluid as heat, giving a sinusoidal temperature rise in the fluid in space and generating counter propagating acoustic waves. The acoustic standing wave acts as a nearly adiabatic sound wave and is referred to as the acoustic mode of wave motion while the slow decay of the sinusoidal temperature increase is known as the thermal mode of wave motion.[16] Both the acoustic and thermal modes of the wave in the grating have associated density changes; hence, a recording of the intensity of diffraction of a continuous "probe" laser beam directed at the Bragg angle to the grating acts as a monitor of the time evolution of the density variations induced by optical excitation. From a knowledge of the optical fringe spacing in the grating, measurements of the oscillation frequency and decay rate of the acoustic wave can be used to determine the sound speed and damping rate of the acoustic wave, while a measurement of the slow decay of the sinusoidal temperature variation gives the thermal diffusivity of the fluid. [12−16]

Here we report a study using the transient grating method[9−16] directed not only at measurement of the physical properties of RTILs but also toward determining the relationship between the RTIL structure and their thermophysical properties. In the Experimental Section, we describe the experimental apparatus, present data, and give expressions for reduction of the data. The Discussion section points out the correlations in the thermophysical properties of the different RTIL samples studied, elucidating the effects of the different anions or cations on the thermophysical properties of the RTILs.

* Corresponding author. Tel: (401)863-3619. E-mail:frez@brown.edu.

10.1021/je0600092 CCC: $33.50
Published on Web 05/13/2006

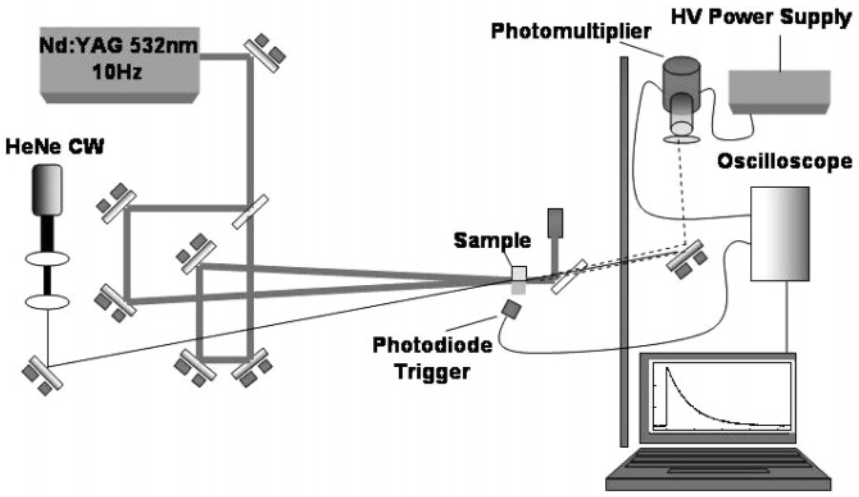

Figure 1. Schematic diagram of the transient grating system.

Table 1. List of Room Temperature Ionic Liquids Used in This Study

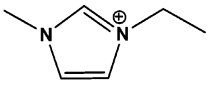	1-ethyl-3-methylimidazolium Tf_2N^- or $[EMIm]^+$ $[Tf_2N]^-$
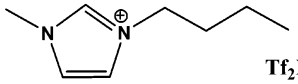	1-butyl-3-methylimidazolium Tf_2N^- or $[BMIm]^+$ $[Tf_2N]^-$
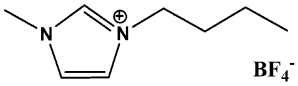	1-butyl-3-methylimidazolium BF_4^- or $[BMIm]^+$ $[BF_4]^-$
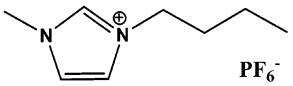	1-butyl-3-methylimidazolium PF_6^- or $[BMIm]^+$ $[PF_6]^-$
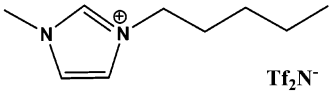	1-pentyl-3-methylimidazolium Tf_2N^- or $[PMIm]^+$ $[Tf_2N]^-$
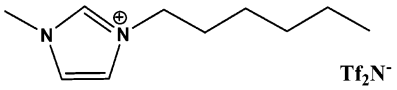	1-hexyl-3-methylimidazolium Tf_2N^- or $[HMIm]^+$ $[Tf_2N]^-$
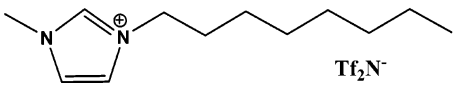	1-octyl-3-methylimidazolium Tf_2N^-or $[OMIm]^+$ $[Tf_2N]^-$

Experimental Section

Instrument and Methods. The transient grating apparatus used here is similar to that described by previous researchers,[9] except that a relatively long laser pulse and a small crossing angle are used for the pump beams. As shown in Figure 1, the frequency doubled 532 nm; 10 ns output of a Q-switched Nd:YAG laser operated at 10 Hz was used as the pump beam. The 532 nm beam was split into two equal intensity beams by a beam splitter and recombined to produce approximately 100 μm optical fringes in a 1.0 cm × 1.0 cm × 4.5 cm glass cuvette. A continuous, 4 mW, 633 nm He−Ne laser beam was directed at the Bragg angle, θ_B, to the grating where θ_B satisfies

$$\sin \theta_B = \lambda_{probe}/2\Lambda \quad (1)$$

where Λ is the fringe spacing of the grating and λ_{probe} is the wavelength of the probe beam. A side-on photomultiplier (Hamamatsu, Inc. model R928) whose output was fed to an inverting operational amplifier (Burr-Brown Inc., model OPA686) was used to detect the first-order diffracted beam. The photomultiplier was equipped with a narrow band interference filter to block scattered radiation from the pump laser. Signals from the photomultiplier were averaged with a 1.5 GHz bandwidth (Agilent, Inc., model 545845) digitizing oscilloscope.

The pump laser beam could be attenuated with a half wave plate and Glan Taylor polarizer to give pulse energies of the order of 10 mJ pulses at the front surface of the cuvette. In experiments with $[BMIm]^+[PF_6]^-$, laser pulse energies were on the order of 33 mJ. (See Table 1 for structures of the RTILS used in this study.) Experiments were carried out over a range of pulse energies to determine if the recorded waveforms were affected by laser pulse energy. Because the RTIL samples are transparent at 532 nm, an absorbing dye tris(1,10-phenanthroline) iron(II) sulfate known as ferroin was added to each sample.

Specifically, 1.0 μL of 0.025 mol·L^{-1} aqueous ferroin solution was added to 2 mL of each RTIL sample. A control experiment was carried out with $[BMIm]^+[BF_4]^-$, which has a small absorbance so that a transient grating experiment could be done without the addition of a dye. The results of the experiment agreed, within the experimental error, with a measurement on the same RTIL containing the 1.0 μL ferroin dye solution used with the other RTILs.

Experiments were conducted first to determine the fringe spacing, performed by using a solution of $CoCl_2$ in methanol whose sound speed is well-documented.[17] The acoustic wavelength Λ (related to the wavenumber K through $K = 2\pi/\Lambda$) for two different angles of intersection of the pump beams was found to be 104 μm and 92 μm. Data for each RTIL sample was taken several times using different laser fluences; data were taken at the two different angles of intersection of the pump beams as well. All experiments were done at 0.1 MPa and 296.85 K.

Chemicals. 1-Methylimidazole (mole fraction purity of 99 %), 1-chlorooctane (mole fraction purity of 99 %), 1-chloropentane (mole fraction purity of 99 %), 1-chlorohexane (mole fraction purity of 99 %), acetonitrile (mole fraction purity of 99 %), ethyl acetate (mole fraction purity of 99 %), lithium trifluoromethane sulfonimide ($LiTf_2N$) (mole fraction purity of 99.95 %), and hexafluorophosphoric acid with a mass fraction of 0.60 in water were purchased from Alfa Aesar. 1-Methylimidazole was distilled under vacuum prior to use. Other chemicals were used as received.

Chloride salts of C_5, C_6, and C_8 alkyl imidazolium were synthesized from corresponding alkyl chloride and 1-methylimidazole based on methods used in our previous studies.[6−8] For example, octylmethylimidazolium chloride was prepared by refluxing a 1:1 molar ratio mixture of 1-methylimidazole and octyl chloride under nitrogen at 333 K for 2 days. Initially, there were two layers in the mixture. As the reaction proceeded, it became one single layer. The product was washed twice with ethyl acetate. The chloride salts were then converted into corresponding $[Tf_2N]^-$ salts by metathesis reaction using the procedure reported in our earlier studies.[6−8] Essentially, a 1:1 molar ratio of alkyl methylimidazolium chloride and $LiTf_2N$ were dissolved in cold water separately. The solutions were then mixed together and stirred for 2 h at room temperature. As the reaction proceeded, the homogeneous solution separated into two layers with a water layer on top and an RTIL layer in the bottom. The upper water layer was discarded; the RTIL was further washed with water three times and then dried under vacuum at 333 K overnight. Similar procedures were used to prepare $[C_4MIm]^+[BF_4]^-$ and $[C_4MIm]^+[PF_6]^-$ from $[C_4MIm]^+[Cl]^-$. Purity of the ionic liquids obtained was verified by ^{1}H NMR. The chemical shifts agree with previous research.[18−24] Although a reference is not available for $[PMIm]^+[Tf_2N]^-$, the NMR spectra is in excellent agreement with the expected characteristic peaks of this RTIL. The NMR characteristics of each compound are as follows:

$[BMIm]^+[BF_4]^-$ ^{1}H NMR (DMSO-d_6, 300 MHz). δ: 9.06 (1H, s), 7.73 (1H, t), 7.67 (1H, t), 4.13 (2H, t), 3.82 (3H, s), 1.74 (2H, m), 1.24 (2H, m), 0.88 (3H, t).

$[BMIm]^+[PF_6]^-$ ^{1}H NMR (DMSO-d_6, 300 MHz). δ: 9.06 (1H, s), 7.73 (1H, t), 7.66 (1H, t), 4.13 (2H, t), 3.82 (3H, s), 1.74 (2H, m), 1.24 (2H, m), 0.88 (3H, t).

$[BMIm]^+[Tf_2N]^-$ ^{1}H NMR (DMSO-d_6, 300 MHz). δ: 9.09 (1H, s), 7.74 (1H, t), 7.67 (1H, t), 4.15 (2H, t), 3.83 (3H, s), 1.75 (2H, m), 1.25 (2H, m), 0.89 (3H, t).

$[EMIm]^+[Tf_2N]^-$ ^{1}H NMR (DMSO-d_6, 300 MHz). δ: 9.09 (1H, s), 7.75 (1H, s), 7.66 (1H, s), 4.18 (2H, q), 3.83 (3H, s), 1.41 (3H, t).

$[PMIm]^+[Tf_2N]^-$ ^{1}H NMR (DMSO-d_6, 300 MHz). δ: 9.08 (1H, s), 7.74 (1H, t), 7.67 (1H, t), 4.13 (2H, t), 3.82 (3H, s), 1.76 (2H, m), 1.28 (2H, m), 1.19 (2H, m), 0.85 (3H, t).

$[HMIm]^+[Tf_2N]^-$ ^{1}H NMR (DMSO-d_6, 300 MHz). δ: 9.07 (1H, s), 7.74 (1H, t), 7.67 (1H, t), 4.13 (2H, t), 3.82 (3H, s), 1.76 (2H, m), 1.25 (6H, broad), 0.84 (3H, t).

$[OMIm]^+[Tf_2N]^-$ ^{1}H NMR (DMSO-d_6, 300 MHz). δ: 9.07 (1H, s), 7.74 (1H, t), 7.67 (1H, t), 4.12 (2H, t), 3.82 (3H, s), 1.76 (2H, m), 1.23 (10H, broad), 0.84 (3H, t). Complete NMR spectra of all seven ionic liquids are presented in the Supporting Information.

Data Reduction. The theory governing the photoacoustic effect and its application to the transient grating technique have been described previously.[10−16] The density change in the grating δ can be written as

$$\delta = \frac{\bar{a}E_0\beta}{C_p}[-e^{-K^2\alpha t} + e^{-K^2\sigma t}\cos(cKt)] \quad (2)$$

where the damping parameter σ and the viscous and heat conduction lengths[16] l_v' and l_h, respectively, are given by

$$\sigma = \frac{1}{2}c[l_v' - (\gamma - 1)l_h]$$

$$l_v' = \frac{\eta + \frac{4}{3}\mu}{\rho c}$$

$$l_h = \frac{\chi}{c} \quad (3)$$

The quantities α, c, γ, η, μ, and ρ are the thermal diffusivity, sound speed, heat capacity ratio, bulk viscosity coefficient, shear viscosity coefficient, and density of the fluid, respectively. E_0, $\bar{a}$, β, and C_p are the energy fluence of the laser beam, the optical absorption coefficient, the volume expansion coefficient, and the isobaric heat capacity, respectively, of the fluid. The first and second terms in eq 2 describe the time dependences of the thermal and acoustic modes of wave motion, respectively. Since the decays of the acoustic and thermal mode densities back to their ambient values take place on such different time scales, they were recorded on the oscilloscope using different time bases. The fast oscillations of the acoustic mode were not visible on the long time base used for recording the thermal mode; hence, the diffracted light intensity recorded by the photomultiplier, represented by I_A and I_T for the two different modes, were fitted separately with the following two expressions:

$$I_A(t) = \left(F\left\{-A + e^{-E(t+C)}\cos\left[\frac{2\pi(t+C)}{B}\right]\right\}\right)^2 + D_1 \quad (4)$$

$$I_T(t) = [-G\,e^{-H(t+C)}]^2 + D_2 \quad (5)$$

where the quantities denoted by capital letters are adjustable parameters used in the least-squares fitting procedure. In the data fitting, the thermal mode contribution to the signal on a short time scale is approximated as -1 in eq 4, as its decay is negligible on a short time scale. Figures 2 and 3 show an experimental waveform for the ionic liquid $[BMIm]^+$ $[BF_4]^-$ and their least-squares fits using eq 4.

To ensure the accuracy of the technique and the reliability of the fitting model, calibration experiments were performed

Table 2. Experimental Thermal Diffusivities (α), Sounds Speeds (*c*), and Damping Parameters (*σ*) of Ionic Liquids Compared with Literature Sound Speeds and Viscosities

	10^{-7} α	*c*	c_{Ref}/(m·s^{-1})	10^{-4} *σ*	*η*/(mPa·s)	
ionic liquid	m^2·s^{-1}	m·s^{-1}	*p* = 0.1 MPa *T* = (293.15 ± 0.01) K	m^2·s^{-1}	*T*/K	
[BMIm]$^+$ [BF$_4$]$^-$	0.86 ± 0.01	1564 ± 8	1570 ± 3[a]	3.7 ± 0.4	298	119.78 ± 1.28[d]
[BMIm]$^+$[PF$_6$]$^-$	0.75 ± 0.02	1441 ± 4	1433 ± 3[a]	4.2 ± 0.4	298	207.00 ± 11.12[c]
[BMIm]$^+$[Tf$_2$N]$^-$	0.60 ± 0.01	1227 ± 6	1238.06 ± 62[b]	2.4 ± 0.6	293.15	52 ± 3[c]
[EMIm]$^+$[Tf$_2$N]$^-$	0.601 ± 0.004	1240 ± 4		2.6 ± 0.7	293.15	31[c]
[PMIm]$^+$[Tf$_2$N]$^-$	0.58 ± 0.02	1227 ± 2		3.0 ± 0.8		
[HMIm]$^+$[Tf$_2$N]$^-$	0.606 ± 0.009	1232 ± 11		2.3 ± 0.3		
[OMIm]$^+$[Tf$_2$N]$^-$	0.61 ± 0.01	1232 ± 5		3.1 ± 0.7		

[a] The literature values were taken from ref 26. [b] The literature values were taken from ref 27. [c] The literature values were taken from ref 2. [d] The literature values were taken from ref 28.

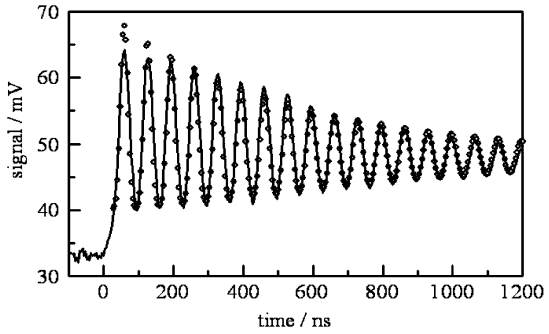

Figure 2. Photomultiplier signal vs time for an experiment with [BMIm]$^+$[BF$_4$]$^-$ showing the acoustic mode of wave motion. The solid trace is the experimental signal and the circles are the model fit using eq 4.

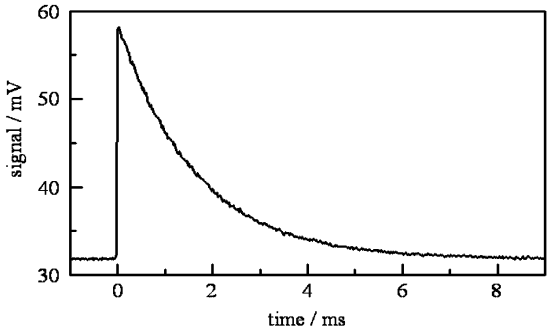

Figure 3. Photomultiplier signal vs time for an experiment with [BMIm]$^+$[BF$_4$]$^-$ showing the thermal mode of wave motion. The ratio of the standard deviation of the fit to the least squares value of the thermal diffusivity is 0.01.

using $CoCl_2$ in methanol (with an absorbance less than 0.3 cm^{-1}) as a standard. It was found that the thermal diffusivity of methanol determined by the transient grating method was found to be (1.00 ± 0.03)·10^{-7} m^2·s^{-1} and is in excellent agreement with ref 17. In measurements on the RTILs, data were taken at grating fringe spacings of 104 μm and 92 μm (i.e., with wavenumbers of 6.0·10^4 m^{-1} and 6.8·10^4 m^{-1}, respectively). The data for each chemical species listed in Table 2 are averages from experiments taken with different laser energy fluences and fringe spacings.

The discrepancies in thermal diffusivities and sound speeds of the RTILs had no dependence on changes in either laser energy fluence or fringe length. Typically, the percent relative standard deviation of the experiments for each RTIL in determining the thermal diffusivity is better than ± 4 % and in determining the sound speed is better than ± 0.5 %. The standard deviations of the data are reported in Table 2. Some of the uncertainties and conditions of the reference values were not found in the literature.

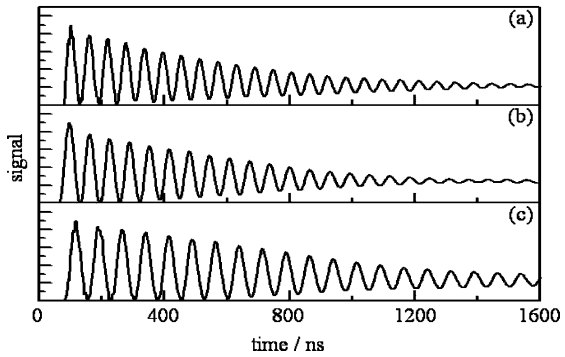

Figure 4. Photomultiplier signal (in arbitrary units) vs time for three RTILs: (a) [BMIm]$^+$[BF$_4$]$^-$; (b) [BMIm]$^+$[PF$_6$]$^-$; and (c) [BMIm]$^+$[Tf$_2$N]$^-$.

Results and Discussion

The results listed in Table 2 show that the properties of the anion of the RTILs have a strong effect on the sound speed; specifically, changing the anion from [BF$_4$]$^-$ to either [PF$_6$]$^-$ or [Tf$_2$N]$^-$ leads to a decrease in the sound speeds, from (1564 ± 8) m·s^{-1} for [BMIm]$^+$[BF$_4$]$^-$ to (1441 ± 4) m·s^{-1} for [BMIm]$^+$[PF$_6$]$^-$ and to (1227 ± 6) m·s^{-1} for [BMIm]$^+$[Tf$_2$N]$^-$. A change of the cation in these species, on the other hand, does not show a significant affect on the sound speed of the RTILs: the sound speed of the RTILs with C_2MIm cations (i.e., [EMIm]$^+$[Tf$_2$N]$^-$ (1240 ± 4) m·s^{-1}) is similar to that for RTILs with C_4MIm cations ([BMIm]$^+$[Tf$_2$N]$^-$ (1227 ± 6) m·s^{-1}), C_5MIm cations ([PMIm]$^+$[Tf$_2$N]$^-$ (1227 ± 2) m·s^{-1}), C_6MIm cations ([HMIm]$^+$[Tf$_2$N]$^-$ (1232 ± 11) m·s^{-1}), and C_8MIm cations ([OMIm]$^+$ [Tf$_2$N]$^-$ (1232 ± 5) m·s^{-1}). Generally, it would be expected that an increase in size of the cation by lengthening the alkyl chain would increase the viscosity and hence the damping of the acoustic mode.[2,25] Although, the use of the damping constant appears to be an effective indicator for measuring large viscosity changes, it does not appear to discern between small changes in viscosity. More experiments with different RTILs are required for an accurate assessment. It is noteworthy that the sound speeds reported here for [BMIm]$^+$[BF$_4$]$^-$ and [BMIm]$^+$[PF$_6$]$^-$ agree to within ± 8 m·s^{-1} with the results determined by other workers[26] using an acoustic microcell operating at 0.5 MHz.

As can be seen by inspection of Figure 4, the damping constant for [BMIm]$^+$[PF$_6$]$^-$ is similar to that of [BMIm]$^+$[BF$_4$]$^-$ but is approximately double that of [BMIm]$^+$[Tf$_2$N]$^-$. As Table 2 shows, the character of the anion of the RTIL has a strong effect on the damping parameter *σ*, while that of the cation exerts no significant effect—a trend that parallels the relative influence of the anion and cation on the sound speed, as noted above. Since *σ* is a decay parameter that includes energy losses primarily due to viscosity with typically only a small contribution from heat conduction, the data suggest that for identical

Table 3. Experimentally Determined Thermal Conductivities (λ) of $[BMIm]^+[BF_4]^-$, $[BMIm]^+[PF_6]^-$, $[BMIm]^+[Tf_2N]^-$, and $[EMIm]^+[Tf_2N]^-$ from Previously Reported Values of Density (ρ) and Specific Heat Capacity (C_p)[a]

	ρ/(kg·m^{-3})			C_p/(J·kg^{-1}·K^{-1})		λ_{Ref}/(W·m^{-1}·K^{-1})
ionic liquid	p/MPa	T/K		p = 0.1 MPa T = 298.15 K	λ/(W·m^{-1}·K^{-1})	T = 298 K
$[BMIm]^+[BF_4]^-$	0.1	298.15	1205.0 ± 0.2[b]	1613 ± 81[b]	0.162 ± 0.006	0.186 ± 0.001[f]
		295.4	1205 ± 2[e]	1555 ± 58[e]		
		293.15	1201.8[f]	1614[g]		
$[BMIm]^+[PF_6]^-$	0.1	298.15	1366.0 ± 0.3[b]	1438 ± 72[b]	0.109 ± 0.005	
		298	1363[d]	1399 ± 62[e]		
$[BMIm]^+[Tf_2N]^-$	0.1	298.15	1437.04[c]	1293[c]	0.108 ± 0.004	
		295	1429[d]	1279 ± 46[e]		
		296.4	1438.6 ± 0.3[e]			
$[EMIm]^+[Tf_2N]^-$		295	1520[d]	1340 ± 52[e]	0.120 ± 0.005	
		296.0	1521±2[e]	1291[g]		

[a] The thermal conductivities presented by this work were calculated from the averages of the literature heat capacities and literature densities. [b] The literature values were taken from ref 26. [c] The literature values were taken from ref 27. [d] The literature values were taken from ref 2. [e] The literature values were taken from ref 5. [f] The literature values were taken from ref 28. [g] The literature values were taken from ref 29.

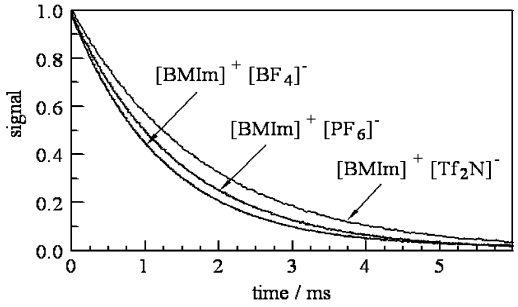

Figure 5. Photomultiplier signal vs time for three RTILs. The signal for all three traces is scaled to unity at time = 0. The thermal diffusivities of the RTILs can be seen to decrease with the size of the anion.

densities that $[BMIm]^+[PF_6]^-$ is the most viscous of the RTILs studied here and that varying the number of carbons on the cation has little influence on the overall viscosity. Furthermore, if the bulk viscosity can be taken as negligible to the shear viscosity, then the experimental quantity σ is related to the bulk and shear viscosities through $\sigma = (2/3)\cdot\mu\cdot\rho$. As listed in Table 2, viscosities for $[BMIm]^+[PF_6]^-$, $[BMIm]^+[Tf_2N]^-$, and $[EMIm]^+[TF_2N]^-$ are reported[2] to be 207 mPa·s, 52 mPa·s, and 31 mPa·s, respectively. This mirrors the trend for σ determined from the experiments reported here.

As in the case of the sound speed and damping, the character of the anion in an RTIL exerts strong influence on thermal diffusivity. The effect of changing anion can be seen in Figure 5, which plots the decays of the thermal mode for the three RTILs with the same cation but with different anions. It is evident that the decay of the thermal mode becomes slower as the anion increases in bulk.

Although, the transient grating measurements yield values for thermal diffusivity for each RTIL directly, the thermal conductivity must be found from a knowledge of the density and specific heat capacity through the relation $\alpha = \lambda\cdot\rho^{-1}\cdot C_p^{-1}$. Only a few values of density and heat capacity have been reported for $[BMIm]^+[BF_4]^-$, $[BMIm]^+[PF_6]^-$, $[BMIm]^+[Tf_2N]^-$, and $[EMIm]^+[Tf_2N]^-$.[2,5,26−29] Based on the reported values of these two quantities, thermal conductivities for these four RTILs were calculated, and the results listed in Table 3.

In summary, we have reported values for the sound speed, acoustic damping, and thermal diffusivities of several RTILs. The relative ease of determining these parameters, the small error found in the resulting data fits, and the agreement of some of the extracted parameters with conventional methods reaffirms the value of the transient grating method for determining thermophysical parameters of fluids.

Supporting Information Available:

The complete H^1 NMR spectra of the seven RTILs reported in this work. This material is available free of charge via the Internet at http://pubs.acs.org.

Literature Cited

(1) Welton, T. Room-temperature ionic liquids. Solvents for synthesis and catalysis. *Chem. Rev.* **1999**, *99*, 2071−2084.
(2) Mantz, R. A.; Trulove, P. C. *Ionic Liquids in Synthesis*; Wasserscheid, P., Welton, T., Eds.; Wiley-VCH: Weinheim, Germany, 2003.
(3) Holbrey, J. D.; Reichart, W. M.; Reddy, R. G.; Rogers, R. D. *Ionic Liquids as Green Solvents*; Seddon, K. R., Rogers, R. D., Eds.; ACS Symposium Series 856; American Chemical Society: Washington, DC, 2003.
(4) Ohno, H. *Electrochemical Aspects of Ionic Liquids*; John Wiley: New York, 2005.
(5) Fredlake, C. P.; Crosthwaite, J. M.; Hert, D. G.; Aki, N. V. K.; Brennecke, J. Thermophysical properties of imidazolium-based ionic liquids. *J. Chem. Eng. Data* **2004**, *49*, 954−964.
(6) Tran, C. D.; De Paoli Lacerda, S. H.; Oliveira, D. Absorption of water by room-temperature ionic liquids: affect of anions on concentration and states of water. *Appl. Spectrosc.* **2003**, *57*, 152−157.
(7) Tran, C. D.; De Paoli Lacerda, S. H. Determination of binding constants of cyclodextrins in room-temperature ionic liquids by near-infrared spectrometry. *Anal. Chem.* **2002**, *74*, 5337−5341.
(8) Mele, A.; Tran, C. D.; De Paoli Lacerda, S. H. The structure of a room-temperature ionic liquid with and without trace amounts of water: the role of C−H···O and C−H···F interactions in 1-*n*-butyl-3-methylimidazolium tetrafluoroborate. *Angew. Chem., Int. Ed.* **2003**, *42*, 4364−4366.
(9) Mandelis, A. *Non-destructive Evaluation (NDE)*; Prentice Hall: Englewood Cliffs, NJ, 1994.
(10) Mandelis, A. Photothermal diagnostic technologies. *Opt. Photonics News* **2002**, *13*, 32−37.
(11) Eichler, H. J.; Gunther, P.; Pohl, D. W. *Laser-Induced Dynamic Gratings*; Springer: Berlin, 1982.
(12) Yan, Y.-X.: Chen, L.-T.; Nelson, K. A. The temperature-dependent distribution of relaxation times in glycerol: time-domain light scattering study of acoustic and mountain-mode behavior in the 20 MHz−3 GHz frequency range. *J. Chem. Phys.* **1988**, *88*, 6477−6486.
(13) Duggal, A. R.; Nelson, K. A. Picosecond−microsecond structural relaxation dynamics in polypropylene glycol: impulsive stimulated light-scattering experiments. *J. Chem. Phys.* **1991**, *94*, 7677−7688.
(14) Chen, H. X.; Diebold, G. J. Production of the photoacoustic effect and transient gratings by molecular volume changes. *J. Chem. Phys.* **1996**, *104*, 6730−6741.
(15) Sun, T.; Morais, J.; Diebold, G. J.; Zimmt, M. B. Investigation of viscosity and heat conduction effects on the evolution of a transient picosecond photoacoustic grating. *J. Chem. Phys.* **1992**, *97*, 9324−9334.
(16) Morse, P.; Ingard, K. U. *Theoretical Acoustics*; McGraw-Hill: New York, 1968.
(17) Linde, D. R., Ed. *Handbook of Chemistry and Physics*, 85th ed.; CRC Press: New York, 2004; pp 6−214, 14−42, 15−28, 15−21.
(18) Bonhôte, P.; Dias, A.-P.; Papageorgiou, N.; Kalyanasundaram, K.; Grätzel, M. Hydrophobic, highly conductive ambient-temperature molten salts. *Inorg. Chem.* **1996**, *35*, 1168−1178.
(19) Luo, H.; Dai, S.; Bonnesen, P. V.; Buchanan, A. C., III; Holbrey, J. D.; Bridges, N. J.; Rogers, R. D. Extraction of cesium ions from

aqueous solutions using calix[4]arene-bis(*tert*-octylbenzo-crown-6) in ionic liquids. *Anal. Chem.* **2004**, *76*, 3078−3083.
(20) Reynolds, J. L.; Erdner, K. R.; Jones, P. B. Photoreduction of benzophenones by amines in room-temperature ionic liquids. *Org. Lett.* **2002**, *4*, 917−919.
(21) Xu, D.; Liu, B.; Luo, S.; Xu, Z.; Shen, Y. A novel and eco-friendly method for the preparation of ionic liquids. *Synthesis* **2003**, *17*, 2626−2628.
(22) Nockemann, P.; Beurer, E.; Driesen, K.; Van Deun, R.; Van Hecke, K.; Van Meervelt, L.; Binnemans, K. Photostability of a highly luminescent europium β-diketonate complex in imidazolium ionic liquids. *Chem. Commun.* **2005**, 4354−4356.
(23) Amigues, E.; Hardacre, C.; Keane, G.; Migaud, M.; O'Neill, M. Ionic liquids—media for unique phosphorus chemistry. *Chem. Commun.* **2006**, 72−74.
(24) Headley, A. D.; Jackson, N. M. The effect of the anion on the chemical shifts of the aromatic hydrogen atoms of liquid 1-butyl-3-methylimidazolium salts. *J. Phys. Org. Chem.* **2002**, *15*, 52−55.
(25) Buzzeo, M. C.; Evans, R. G.; Compton, R. G. Non-haloaluminate room-temperature ionic liquids in electrochemistry—a review. *Chem. Phys. Chem.* **2004**, *5*, 1106−1120.
(26) de Azevedo, R. G.; Esperanca, J. M. S. S.; Najdanovic-Visak, V.; Visak, Z. P.; Guedes, H. J. R.; da Ponte, M. N.; Rebelo, L. P. N. J. Thermophysical and thermodynamic properties of 1-butyl-3-methylimidazolium tetrafluoroborate and 1-butyl-3-methylimidazolium hexafluorophosphate over an extended pressure range. *J. Chem. Eng. Data* **2005**, *50*, 997−1008.
(27) de Azevedo, R. G.; Esperanca, J. M. S. S.; Szydlowski, J.; Visak, Z. P.; Pires, P. F.; Guedes, H. J. R.; Rebelo, L. P. N. Thermophysical and thermodynamic properties of ionic liquids over an extended pressure range: [bmim][NTf_2] and [hmim][NTf_2]. *J. Chem. Thermodyn.* **2005**, *37*, 888−899.
(28) Van Valkenburg, M. E.; Vaughn, R. L.; Williams, M.; Wilkes, J. S. Thermochemistry of ionic liquid heat-transfer fluids. *Thermochim. Acta* **2005**, *425*, 181−188.
(29) Waliszewski, D.; Stepniak, I.; Piekarski, H.; Lewandowski, A. Heat capacities of ionic liquids and their heats of solution in molecular liquids. *Thermochim. Acta* **2005**, *433*, 149−152.

Received for review January 6, 2006. Accepted April 5, 2006. C.F. and G.J.D. gratefully acknowledge the support of this research by the U.S. Department of Energy under Grant ER-13235.

JE0600092